

Adsorption of rare-gas atoms on Cu(111) and Pb(111) surfaces by van der Waals corrected density functional theory

Pier Luigi Silvestrelli, Alberto Ambrosetti, Sonja Grubisić,* and Francesco Ancilotto

Dipartimento di Fisica e Astronomia, Università di Padova, via Marzolo 8, I-35131 Padova, Italy and DEMOCRITOS National Simulation Center, Istituto Officina dei Materiali, Consiglio Nazionale delle Ricerche, Trieste, Italy
(Received 14 December 2011; revised manuscript received 16 March 2012; published 3 April 2012)

The DFT/vdW-WF method, recently developed to include the Van der Waals interactions in Density Functional Theory (DFT) using the maximally localized Wannier functions, is applied to the study of the adsorption of rare-gas atoms (Ne, Ar, Kr, and Xe) on the Cu(111) and Pb(111) surfaces at three high-symmetry sites. We evaluate the equilibrium binding energies and distances and the induced work-function changes and dipole moments. We find that for Ne, Ar, and Kr on the Cu(111) surface the different adsorption configurations are characterized by very similar binding energies while the favored adsorption site for Xe on Cu(111) is on top of a Cu atom, in agreement with previous theoretical calculations and experimental findings and in common with other close-packed metal surfaces. Instead, the favored site is always the hollow one on the Pb(111) surface, which therefore represents an interesting system where the investigation of high-coordination sites is possible. Moreover, the Pb(111) substrate is subject, upon rare-gas adsorption, to a significantly smaller change in the work function (and to a correspondingly smaller induced dipole moment) than Cu(111). The roles of the chosen reference DFT functional and of different van der Waals corrections as well as their dependence on different rare-gas adatoms are also discussed.

DOI: [10.1103/PhysRevB.85.165405](https://doi.org/10.1103/PhysRevB.85.165405)

PACS number(s): 68.43.Bc, 71.15.Mb, 68.35.Md

I. INTRODUCTION

Understanding adsorption processes on solid surfaces is essential to design and optimize countless material applications and to interpret, for instance, scattering experiments and atomic-force microscopy. In particular, the adsorption of rare-gas (RG) atoms on metal surfaces is prototypical¹ for physisorption processes. Basically, the weak binding of physisorbed closed-electron-shell atoms, such as RG atoms, is due to an equilibrium between attractive, long-range van der Waals (vdW) interactions and short-range Pauli repulsion acting between the electron charge densities of the substrate and the adatoms.²

Up to now RG adsorption on many close-packed metal surfaces such as Ag(111), Al(111), Cu(111), Pd(111), and Pt(111) has been extensively studied both experimentally³⁻⁶ and theoretically,⁶⁻¹⁴ while for Pb it has not, but for the experimental measurements of Ferralis *et al.*¹⁵ and the recent theoretical investigation of Zhang *et al.*,¹⁶ who studied the tribological properties of Ne and Kr on the Pb(111) surface. The Pb surface is important for practical applications: For instance, there is considerable interest in the frictional (tribological) properties of gases on Pb at low temperatures; in particular, Pb is used¹⁵⁻¹⁷ as a material for the electrodes and as adsorption surfaces in nanofriction experiments because it is easy to grow a very uniform film already at room temperature and to remove the surface contaminants deposited over time on the electrodes due to its large diffusion coefficient. The Pb(111) surface also exhibits interesting and unusual properties: For instance, one striking finding is the drastic difference between the sliding friction of Ne and Kr monolayers or multilayers.^{16,17}

In principle, due to the nondirectional character of the vdW interactions that should be the dominant one in physisorption processes, surface sites that maximize the coordination of the RG adsorbate atom were expected to be the preferred

ones, so it was usually assumed that the adsorbate occupies the maximally coordinated hollow site. This assumption was also based on the expectation that the atom in the hollow site would be closer to the surface, thus experiencing a more attractive potential; behind this is the notion that the repulsive potential at the surface is proportional to the atomic charge density and the natural assumption is that the charge density is highest at the locations of the atoms, thus making the top site energetically unfavored. Calculations where the total adatom-substrate interaction is described by the sum of empirical binary potentials, which are widely used and often give reasonable results for adsorption energies, seem to confirm this expectation since the highly coordinated hollow sites naturally emerge as the preferred adsorption sites for the adatoms. However, this picture has been questioned by many experimental³⁻⁵ and theoretical⁸⁻¹¹ studies, which indicate that the actual scenario is more complex. In particular, for Xe and Kr a general tendency is found^{6,8-11} for adsorption on metallic surfaces in the low-coordination top sites (this behavior was attributed^{6,18} to the delocalization of charge density that increases the Pauli repulsion effect at the hollow sites relative to the top site and lifts the potential well upward in both energy and height); for Ar the situation seems to be less clear.⁹ For instance, a comparison of theoretical and experimental results⁶ would suggest that the hollow sites are still favored for Ar on Ag(111).

The importance of polarization effects to determine the favored adsorption sites was pointed out by Da Silva *et al.*,⁹ who studied the interaction of RG adatoms with the Pd(111) surface. In fact, for Xe for instance, the polarization is larger in the on-top site, i.e., the larger induced dipole moment increases the attractive interaction between Xe and the metal surface. Therefore, the dominant mechanisms appear to be polarization-induced attraction and site-dependent Pauli repulsion. The latter, being weaker for the on-top

site, stabilizes on-top adsorption.⁷ Interestingly, in a very recent theoretical study¹⁴ Chen *et al.* investigated the adsorption of Xe on different metal surfaces [Cu(111), Cu(110), Pd(111), and Pt(111)] and attributed the on-top site preference not to differences in the exchange repulsion but rather to a delicate interplay between the electrostatic and kinetic energies.

In spite of this recent substantial progress, the understanding of the interaction of RGs with metal surfaces is not complete yet.⁶ It is not clear, for instance, whether a system exists where high-coordinated sites are always preferred. Moreover, there have been relatively few studies of adsorption geometries for the smaller RGs, although these are probably better candidates for the observation of high-coordination sites due to their reduced polarizability with respect to that of Xe or Kr. In fact, the considerable mismatch between the lattice constants of the smaller RGs and those of most metal surfaces causes most commensurate structures to have multiple atoms per unit cell, so that the characterization and interpretation of such systems is quite complex.

Density functional theory (DFT) is a well-established computational approach to study the structural and electronic properties of condensed matter systems from first principles and in particular to elucidate complex surface processes such as adsorptions, catalytic reactions, and diffusive motions. Although current density functionals are able to describe quantitatively condensed matter systems at much lower computational cost than other first-principles methods, they fail¹⁹ to properly describe dispersion interactions. Dispersion forces originate from correlated charge oscillations in separate fragments of matter and the most important component is represented by the R^{-6} vdW interaction,²⁰ originating from correlated instantaneous dipole fluctuations, which plays a fundamental role in adsorption processes of fragments weakly interacting with a substrate (physisorbed).

This is clearly the case for the present systems, which can be divided into well-separated fragments (RG atoms and the metal substrate) with negligible electron-density overlap. The local or semilocal character of the most commonly employed exchange-correlation functionals makes DFT methods unable to correctly predict binding energies and equilibrium distances within both the local density approximation (LDA) and the generalized gradient approximation (GGA).²¹ As a consequence, the basic results often depend, even at a qualitative level, on the adopted DFT functional. For instance, in their *ab initio* study of the interaction of RG adatoms with the Pd(111) surface, Da Silva *et al.*⁹ found that the on-top site preference is obtained by the LDA for all RG adatoms, while the GGA functionals [in the Perdew-Burke-Ernzerhof (PBE) and Perdew-Wang (PW91) schemes] yield the on-top site preference for Xe, Kr, and He adatoms, but the hollow site for Ne and Ar. Typically, in many physisorbed systems GGAs give only a shallow and flat adsorption well at large atom-substrate separations, while the LDA binding energy turns out to be not far from the experimental adsorption energy; however, since it is well known that the LDA tends to overestimate the binding in systems with inhomogeneous electron density (and to underestimate the equilibrium distances), the reasonable performances of LDA must be considered as accidental. Therefore, a theoretical approach beyond the DFT LDA or

GGA framework that is able to properly describe vdW effects is required to provide more quantitative results.⁹

In the past few years a variety of practical methods have been proposed to make DFT calculations able to accurately describe vdW effects (for a recent review see, for instance, Refs. 21 and 22). We have investigated by such a method the adsorption of RG atoms on the Cu(111) and Pb(111) surfaces. The Cu(111) surface has been chosen because of the many experimental and theoretical data available [especially for Xe-Cu(111)], which can be compared with ours in such a way as to validate the present approach. As mentioned above, the less-studied Pb(111) surface could be interesting because, given the relatively large Pb lattice constant (and hence nearest-neighbor surface Pb-Pb distance), it represents a good candidate for a system where RG atoms are preferably adsorbed on hollow sites (the lattice constant of Pb is 4.95 Å, compared to 4.09 Å for Ag, 4.05 Å for Al, 3.92 Å for Pt, 3.89 Å for Pd, and 3.61 Å for Cu).

II. METHOD

In this study we include vdW effects within a standard DFT approach by using the method proposed in Refs. 23–25 (where further details can be found), hereafter referred to as the DFT/vdW-WF method, by introducing an additional term in the exchange-correlation functional as originally proposed by Andersson *et al.*²⁶ to describe the interactions between separate fragments. This contribution, which effectively accounts for the dispersion forces in both the uniform electron gas and separate atom limits, has the form

$$E_{\text{vdW}} = - \sum_{n,l} f_{nl}(r_{nl}) \frac{C_{6nl}}{r_{nl}^6}, \quad (1)$$

with (in a.u.)

$$C_{6nl} = \frac{3}{16\pi^{3/2}} \int_{|\mathbf{r}'| < r'_c} d\mathbf{r}' \int_{|\mathbf{r}| < r_c} d\mathbf{r} \frac{\sqrt{\rho_n(r)\rho_l(r')}}{\sqrt{\rho_n(r) + \sqrt{\rho_l(r')}}}. \quad (2)$$

In the above formulas r_{nl} is the distance between the two separate fragments n and l and $\rho_n(r)$ is the n th fragment electronic density. The cutoff r_c is introduced to remove the divergence of the integral, taking into account that, at small momentum values, the interaction is highly damped.²⁶

In our approach all the fragment densities are conveniently rewritten in terms of the maximally localized Wannier functions (MLWFs) $\{w_n(r)\}$, i.e., $\rho_n(r) = w_n^2(r)$. The MLWFs can be obtained from the occupied Kohn-Sham orbitals, generated by a standard DFT calculation, by means of a unitary transformation that minimizes the functional²⁷

$$\Omega = \sum_n S_n^2 = \sum_n (\langle w_n | r^2 | w_n \rangle - \langle w_n | \mathbf{r} | w_n \rangle^2). \quad (3)$$

The unitary transformation conserves the total density, which is partitioned, however, into single localized fragments, each of them being characterized by its spread S_n and center of mass position r_n . It is therefore possible to express the vdW correction [see Eqs. (1) and (2)] as a sum of single contributions coming from each pair of Wannier functions belonging to different fragments by approximating the shape of the n th Wannier function²⁵ with a H-like exponential.

The DFT/vdW-WF method has already been successfully applied to several systems, including small molecules, bulk, and surfaces;^{23–25,28–30} in particular it allowed us to study the interaction of Ar with graphite and Ar, He, and H₂ with Al surfaces,^{24,25} of water with the Cl- and H-terminated Si(111) surfaces,²⁹ and of RG atoms and water with graphite and graphene.³⁰

We apply here the DFT/vdW-WF method to the case of adsorption of Ne, Ar, Kr, and Xe atoms on the Cu(111) and Pb(111) surfaces. All calculations have been performed with the QUANTUM-ESPRESSO *ab initio* package³¹ (MLWFs have been generated as a postprocessing calculation using the WANT package³²). Similarly to Da Silva *et al.*,⁹ we modeled the clean and RG-covered metal surfaces using a periodically repeated hexagonal supercell, with a $(\sqrt{3} \times \sqrt{3})R30^\circ$ structure and a surface slab made of 15 metal (Cu or Pb) atoms distributed over 5 layers (repeated slabs were separated along the direction orthogonal to the surface by a vacuum region of about 24 Å). The Brillouin zone was sampled using a $6 \times 6 \times 1$ *k*-point mesh. In this model system the RG coverage is 1/3, i.e., one RG adatom for each three metal atoms in the topmost surface layer. The $(\sqrt{3} \times \sqrt{3})R30^\circ$ structure has been indeed observed⁴ at low temperature by low-energy electron diffraction (LEED) for the case of Xe adsorption on Cu(111) and Pd(111) (actually, this is the simplest commensurate structure for RG monolayers on close-packed metal surfaces and the only one for which good experimental data exist) and it was adopted in most of the previous *ab initio* studies.^{7–9,11,12,16} Since the lateral interactions between RG adatoms do not play a critical role in the RG adsorption site preference,⁸ for the sake of simplicity we have used the same structure also for the other RGs (Ne, Ar, and Kr) and in the case of adsorption on Pb(111) as well.

The Pb or Cu surface atoms were kept frozen (of course after a preliminary relaxation of the outermost layers of the clean metal surfaces) and only the vertical coordinates of the RG atoms, perpendicular to the surface, were optimized, this procedure being justified by the fact that only minor surface atom displacements are observed upon physisorption.^{8,16,33} Moreover, the RG atoms were adsorbed on both sides of the slab: In this way the surface dipole generated by adsorption on the upper surface of the slab is canceled by the dipole appearing on the lower surface, thus greatly reducing the spurious dipole-dipole interactions between the periodically repeated images (previous DFT-based calculations have shown that these choices are appropriate^{9,13}). Note that, apparently, in their recent study of Ne and Kr on Pb(111), Zhang *et al.*¹⁶ instead considered adsorption on a single side of the metal slab; the effect of such a choice can be non-negligible, although it depends considerably on the size of the vacuum region and the number of layers included in the reference supercell (five layers in our study, seven in Ref. 16). In fact, in the case of Xe on Pb(111), for instance, we find that the (absolute value of the) binding energy is reduced by 7 meV (about 4%) with respect to that obtained when Xe is adsorbed on both sides of the slab.

We have carried out calculations for various separations of the RG atoms adsorbed on high-symmetry sites, namely, hollow (on the center of the triangle formed by the three surface metal atoms contained in the supercell), top (on the top of a metal atom), and bridge (intermediate between two

nearest-neighbor metal atoms). Actually, two kinds of hollow sites are present: hcp hollow sites, characterized by having atoms directly beneath them in the next layer of atoms, and fcc hollow sites, where this condition does not apply; however, the hcp hollow sites and the fcc hollow sites can be considered equivalent for adsorption because of the small differences in the adsorption properties [for instance, Righi and Ferrario,¹² using the LDA, found a difference of less than 1 meV in the adsorption energy and 0.01 Å in the equilibrium distance for RGs adsorbed on Cu(111)]. For better accuracy, as done in previous applications on adsorption processes,^{24,25,29,30} we have also included the interactions of the MLWFs of the physisorbed fragments not only with the MLWFs of the underlying surface, within the reference supercell, but also with a sufficient number of periodically repeated surface MLWFs (in any case, given the R^{-6} decay of the vdW interactions, the convergence with the number of repeated images is rapidly achieved). Electron-ion interactions were described using norm-conserving pseudopotentials: In the case of Pb and Cu we have explicitly included 14 and 11 valence electrons per atom, respectively (those coming from the $5d^{10}$, $6s^2$, and $6p^2$ atomic orbitals for Pb and $3d^{10}$ and $4s^1$ for Cu). As a reference DFT functional we chose PW91³⁴ because it is widely used in *ab initio* DFT calculations of solids and surfaces and in particular was adopted in several previous simulations¹¹ of Xe interacting with the Cu(111) surface, which facilitates a comparison with the results of the present calculations (note that typically the PW91 gives similar results to that obtained by PBE,³⁵ which represents another popular GGA functional). Using the PW91 functional in test calculations with bulk Pb and Cu, for the equilibrium properties the agreement with experimental estimates is comparable to that found in other DFT calculations.^{8,11,16} In most of our previous applications^{23–25,30} of the DFT/vdW-WF method we adopted the revised PBE (revPBE) functional,³⁶ which turns out to be less accurate than the PW91 functional, to reproduce the basic structural properties of the Cu(111) and Pb(111) surfaces. Nonetheless, tests performed using the revPBE functional indicate that the basic qualitative conclusions, in particular the preferred adsorption site, are not changed; only the quantitative results are affected, as expected since the revPBE functional has a well-known tendency to predict a smaller binding energy than the PW91 or PBE functionals.

By generating the MLWFs for the Cu(111) and Pb(111) substrates, we observe a clear quantitative separation between the spreads of the MLWFs describing *d*-like orbitals and those of the (much more delocalized) MLWFs describing the *s*- and *p*-like orbitals. Moreover, given the high valence-electron density, screening effects are certainly relevant in these metal surfaces. Therefore, at variance with previous calculations,^{24,25,29,30} we have applied the DFT/vdW-WF correction by explicitly considering only the more localized MLWFs corresponding to the *d*-like orbitals, while the *s*- and *p*-like electrons are supposed to give a screening-effect contribution, which is taken into account by following the formulation originally proposed in Ref. 37 to calculate the vdW forces between ions in the noble metals within a simplified model in which the ions are regarded as nonoverlapping and immersed in a uniform electron gas. In Ref. 37 the screening is given in terms of the dielectric function of the electron gas,

which is approximated by the random-phase approximation expression evaluated for the free-electron densities in the noble metals. Here we evaluate the screening effect of the s and p electrons of the substrate by a simpler Thomas-Fermi model in such a way that the vdW correction (the C_6 coefficients) is multiplied by a Thomas-Fermi factor $f_{\text{TF}} = e^{-2(z-z_s)/r_{\text{TF}}}$, where r_{TF} is the Thomas-Fermi screening length relative to the electronic density of a uniform electron gas (jellium model) equal to the average density of the s - and p -like electrons of the present systems, z_s is the average vertical position of the topmost Cu or Pb atoms, and z is the vertical position, measured with respect to z_s , of the adatom. In practice it turns out that only the topmost metal layer gives a relevant contribution, while the effects of the other ones are dramatically reduced by the exponential factor, in line with the common expectation about screening effects in metal surfaces.³⁷ This observation can be exploited to considerably reduce the computational cost of the vdW correction since really only the topmost MLWFs must be taken into account. Clearly our model for describing the screening of the vdW interactions, whose main effect is a considerable reduction of the values of the effective C_6 coefficients, is a crude one; in principle, a more appropriate formulation for modeling adsorbates on metallic surfaces, by incorporating screening effects, would be that put forth by Lifshitz and further developed by Zaremba and Kohn³⁸ (for a recent implementation see, for instance, Ref. 39).

III. RESULTS AND DISCUSSION

In Tables I–VI results are reported for all the systems under consideration, for adsorption on hollow, top, and bridge sites. The binding energy E_b is defined as

$$E_b = 1/2[E_{\text{tot}} - (E_s + 2E_{\text{RG}})], \quad (4)$$

where $E_{s,\text{RG}}$ represent the energies of the isolated fragments (the substrate and the RG atoms, respectively) and E_{tot} is the energy of the interacting system, including the vdW correction term (the factors 2 and 1/2 are due to the adsorption of RG atoms on both sides of the slab); E_s and E_{RG} are evaluated using the same supercell adopted for E_{tot} .

One should point out that the experimentally measured adsorption energy E_a includes not only the interaction of RG atoms with the substrate but also lateral, vdW RG-RG interactions;¹³ however, in most previous calculations the mostly attractive lateral interaction contribution was not considered. As pointed out, for instance, by Lee *et al.*,⁴⁰ who studied n -butane on transition-metal surfaces (another typical weak physisorption system where the vdW interaction is the only attractive force between the nonpolar molecule and the substrate), lateral adatom-adatom interaction energies can be as large as 25% of the total adsorption energy at full coverage. Here E_a is defined as

$$E_a = E_b + (E_l - E_f), \quad (5)$$

where E_l is the total energy (per atom) of the two-dimensional RG lattice [which is as in the adsorption configurations but without the substrate and including vdW RG-RG corrections when the DFT/vdW-WF method is used] and E_f is the energy of an isolated (free) RG atom. Clearly the quantity in parentheses in the above formula represents the lateral

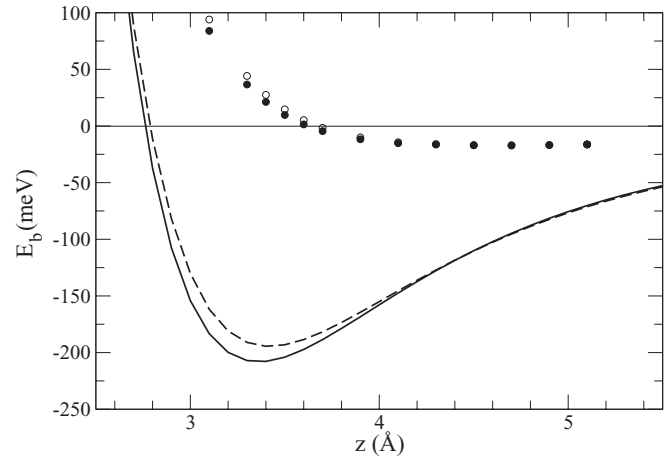


FIG. 1. Binding energy of Xe on Cu(111) in the top and hollow configurations using pure PW91 (full and empty circles, respectively) and DFT/vdW-WF (solid and dashed lines, respectively), as a function of the distance z from the surface.

adatom-adatom interaction energy (per atom). Note that, in their DFT study of Ne and Kr on Pb(111), Zhang *et al.*¹⁶ seem instead to identify E_a with E_b .

The binding energy E_b has been evaluated for several adsorbate-substrate distances; then the equilibrium distances and the corresponding binding energies were obtained by fitting the calculated points with the function $A e^{-Bz} - C_3/(z - z_0)^3$, with A , B , C_3 , and z_0 being adjustable parameters [as illustrated for the Xe-Cu(111) and Xe-Pb(111) cases in Figs. 1 and 2, respectively]. Typical uncertainties in the fit are of the order of 0.05 Å for the distances and a few meV for the minimum binding energies. Our results are compared to available theoretical and experimental estimates and to corresponding data obtained using a pure PW91 functional, the simple LDA functional, and the seamless vdW-DF method of Dion *et al.*⁴¹ (note that the vdW-DF method also has been used in the recent DFT study of Zhang *et al.*¹⁶). As can be seen in Figs. 1 and 2 and Tables I and II, the effect of the vdW

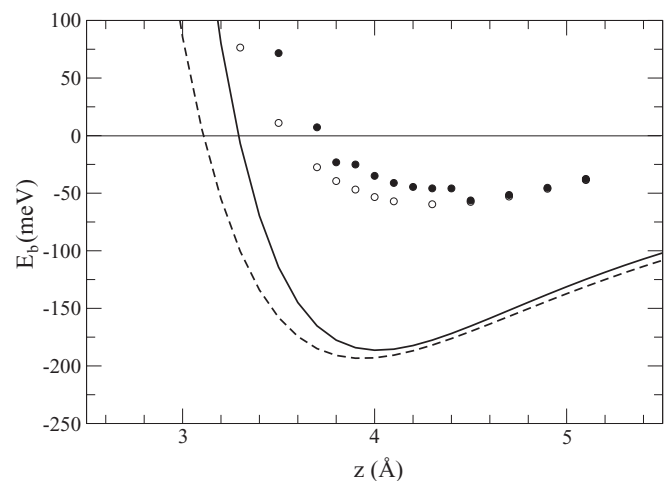


FIG. 2. Binding energy of Xe on Pb(111) in the top and hollow configurations using pure PW91 (full and empty circles, respectively) and DFT/vdW-WF (solid and dashed lines, respectively), as a function of the distance z from the surface.

TABLE I. Binding energy E_b (in meV) of RG atoms on the Cu(111) surface computed using the standard DFT PW91 calculation and including the vdW corrections using our DFT/vdW-WF method, compared to the LDA result, the vdW-DF method by Dion *et al.* (Ref. 41), and available theoretical and experimental (in parentheses) reference data.

System	PW91	DFT/vdW-WF	LDA	vdW-DF	Reference data
Ne-Cu(111) hollow	-17.6	-31.6	-55.7	-56.1	
Ne-Cu(111) top	-17.5	-31.1	-55.4	-55.9	
Ne-Cu(111) bridge	-17.6	-31.0	-55.3	-56.1	
Ar-Cu(111) hollow	-13.0	-67.8	-88.9	-106.6	
Ar-Cu(111) top	-13.0	-71.9	-94.5	-106.3	-85 ^a
Ar-Cu(111) bridge	-13.0	-70.6	-89.4	-106.4	
Kr-Cu(111) hollow	-20.3	-134.2	-117.6	-135.7	
Kr-Cu(111) top	-20.3	-131.1	-126.0	-135.8	-119 ^a
Kr-Cu(111) bridge	-20.3	-130.0	-118.4	-135.7	
Xe-Cu(111) hollow	-22.9	-194.5	-199.3	-167.4	-276, ^b -268 ^c
Xe-Cu(111) top	-23.1	-208.1	-221.9	-167.7	-280, ^b -183, ^a -277, ^c -270 ^d (-190 ^e)
Xe-Cu(111) bridge	-17.1	-191.2	-201.0	-167.4	-278 ^b

^aReference 2.

^bReference 11.

^cReference 4.

^dReference 14.

correction computed by the DFT/vdW-WF method is a much stronger bonding than with a pure PW91 scheme, with the formation of a clear minimum in the binding-energy curve at a shorter equilibrium distance. In spite of the clear shortcomings of the pure PW91 scheme, in general the preferred adsorption site seems to be correctly determined by the latter, although the differences between the binding energies of the different adsorption sites are very small.

We have also computed E_a (assuming a full monolayer coverage of RGs) in the case of Xe on Cu(111), where a RG overlayer in the $(\sqrt{3} \times \sqrt{3})R30^\circ$ structure is experimentally found,⁴ and in the case of Xe on Pb(111), where the formation of a commensurate Xe monolayer was also observed.¹⁵ As can be seen in Table III, all the methods but the pure PW91 scheme correctly predict a smaller E_a on Pb(111) than on Cu(111), although the quantitative results depend considerably on the adopted scheme. In fact, the pure PW91 scheme clearly underestimates E_a , the DFT/vdW-WF and vdW-DF

methods give comparable results, while the LDA is close to the DFT/vdW-WF and vdW-DF methods for Xe on Cu(111) but underestimates for Xe on Pb(111): This can be explained by the fact that the LDA is not able to describe properly the lateral interactions of Xe adatoms that are farther from each other on Pb(111) than on Cu(111). Considering the differences between the binding energies reported in Tables I and II and the adsorption energies listed in Table III, which correspond to the energy of the lateral interactions, one can see that this is small for Xe on Pb(111) (about 6% of the binding energy using the DFT/vdW-WF method) but significantly larger for Xe on Cu(111) (about 46% of the binding energy using the DFT/vdW-WF method) due to the smaller lattice constant of Cu [and consequent shorter Xe-Xe distances of the adsorbed Xe atoms assuming a $(\sqrt{3} \times \sqrt{3})R30^\circ$ structure].

Concerning the adsorption on the Cu(111) surface (see Table I), all the methods used predict that the top configuration

TABLE II. Binding energy E_b (in meV) of RG atoms on the Pb(111) surface computed using the standard DFT PW91 calculation and including the vdW corrections using our DFT/vdW-WF method, compared to the LDA result, the vdW-DF method by Dion *et al.* (Ref. 41), and available theoretical reference data.

System	PW91	DFT/vdW-WF	LDA	vdW-DF	Reference data
Ne-Pb(111) hollow	-31.2	-59.8	-49.4	-71.4	-51.6 ^a
Ne-Pb(111) top	-27.8	-49.1	-42.9	-63.3	-46.8 ^a
Ne-Pb(111) bridge	-19.8	-58.5	-49.1	-64.6	
Ar-Pb(111) hollow	-23.5	-82.4	-78.3	-100.8	
Ar-Pb(111) top	-22.1	-75.0	-64.2	-95.3	
Ar-Pb(111) bridge	-22.7	-84.5	-76.6	-100.1	
Kr-Pb(111) hollow	-30.8	-132.8	-98.8	-136.9	-134.9 ^a
Kr-Pb(111) top	-29.1	-109.8	-81.6	-130.9	-125.1 ^a
Kr-Pb(111) bridge	-24.0	-126.8	-96.7	-136.1	
Xe-Pb(111) hollow	-59.6	-193.5	-142.0	-192.2	-172.6 ^a
Xe-Pb(111) top	-56.3	-186.4	-116.1	-186.4	
Xe-Pb(111) bridge	-52.7	-188.9	-138.6	-191.2	

^aReference 16.

TABLE III. Adsorption energy E_a (see the text for the definition) (in meV) of Xe atoms on the Cu(111) and Pb(111) surfaces computed using the standard DFT PW91 calculation and including the vdW corrections using our DFT/vdW-WF method, compared to the LDA result, the vdW-DF method by Dion *et al.* (Ref. 41), and available experimental (in parentheses) reference data.

System	PW91	DFT/vdW-WF	LDA	vdW-DF	Reference data
Xe-Cu(111) hollow	-51.4	-289.3	-297.3	-268.9	
Xe-Cu(111) top	-51.6	-302.9	-319.9	-269.2	(-227 ^a)
Xe-Cu(111) bridge	-45.6	-286.0	-299.0	-268.9	
Xe-Pb(111) hollow	-62.5	-205.5	-147.9	-252.2	(-191 ^a)
Xe-Pb(111) top	-59.2	-198.4	-122.0	-246.4	
Xe-Pb(111) bridge	-55.6	-200.9	-146.9	-251.2	

^aReference 15.

is energetically favored in the case of Xe, while for Ne, Ar, and Kr the differences among the binding energies of the different adsorption configurations are quite small (using the vdW-DF method, the same is true also for Xe); since these differences are probably comparable to the expected accuracy of the calculations, a precise assignment of the favored adsorption site is not possible. In contrast, the hollow configuration is instead clearly favored by all the methods (see Table II) in the case of the adsorption on Pb(111) of all the considered RG atoms [actually, with DFT/vdW-WF, for Ar on Pb(111) the bridge site appears to be lower in energy; however, given the small difference with the energy of the hollow site, this result should not be overemphasized]. As far as the preferred RG adsorption site is concerned, the Pb(111) surface is similar to graphite/graphene where the hollow site is also energetically favored.^{30,42,43} Our results for Pb(111) are in qualitative agreement with those of Zhang *et al.*,¹⁶ who predict that Ne and Kr indeed prefer high-coordination hollow sites. Note that the energy difference between the hollow and top sites increases by subsequently considering

the PW91, vdW-DF, DFT/vdW-WF, and LDA methods (see also the results of Da Silva *et al.*⁸).

Interestingly, in the case where several experimental reference values are available, namely, Xe on Cu(111), our DFT/vdW-WF method performs better (considering both the binding and adsorption energies and the equilibrium distance; see Tables I, III, and IV) than all the other schemes. In fact, the LDA gives reasonable binding energies but underestimates the equilibrium distances, while the vdW-DF method underestimates the binding energies and overestimates the equilibrium distances, in line with the behavior reported for systems including a metallic surface.⁴⁴ Also note that at a variance with the experimental findings, the vdW-DF method predicts that the top site (see Table I) is only marginally favored (and the distance only marginally different) over the hollow ones; in general, for all the RG atoms on Cu(111) the vdW-DF method gives almost identical binding energies for the top and hollow adsorption sites. In the case of RGs on Pb(111), the hollow structure is favored also by the vdW-DF method, although the difference in the binding energy with respect to

TABLE IV. Equilibrium RG adatom-surface distance (in angstroms) on the Cu(111) surface computed using the standard DFT PW91 calculation and including the vdW corrections using our DFT/vdW-WF method, compared to the LDA result, the vdW-DF method by Dion *et al.* (Ref. 41), and available theoretical and experimental (in parentheses) reference data; the sum s of the vdW radii of the RG atom and the Cu atom is also reported.

System	PW91	DFT/vdW-WF	LDA	vdW-DF	Reference data	s
Ne-Cu(111) hollow	3.90	3.59	3.10	3.70		2.94
Ne-Cu(111) top	3.90	3.57	3.09	3.68		2.94
Ne-Cu(111) bridge	3.90	3.60	3.10	3.68		2.94
Ar-Cu(111) hollow	4.50	3.48	3.19	3.90		3.28
Ar-Cu(111) top	4.50	3.45	3.15	3.86	3.53 ^a	3.28
Ar-Cu(111) bridge	4.50	3.43	3.19	3.86		3.28
Kr-Cu(111) hollow	4.50	3.32	3.21	3.99		3.42
Kr-Cu(111) top	4.50	3.36	3.17	3.99		3.42
Kr-Cu(111) bridge	4.50	3.35	3.20	3.99		3.42
Xe-Cu(111) hollow	4.70	3.42	3.00	4.10	3.40, ^b 3.31 ^c	3.56
Xe-Cu(111) top	4.40	3.36	2.90	4.09	3.45, ^b 3.2, ^d 3.25, ^c 4.0 ^e (3.60 ^f)	3.56
Xe-Cu(111) bridge	4.70	3.41	3.00	4.10		3.56

^aReference 2.

^bReference 13.

^cReference 7.

^dReference 11.

^eReference 14.

^fReference 4.

the top site is smaller than with the present DFT/vdW-WF scheme [the difference was instead larger (see the last column of Table II) in the study of Zhang *et al.*,¹⁶ who used the vdW-DF method but with a reference DFT functional differing from ours by the exchange term]. In the case of Ar on Cu(111) and Pb(111), we observe that our computed binding energies compare favorably with the estimates obtained, using a simple Lennard-Jones potential, by Cheng *et al.*,⁴⁵ who predicted a binding energy between -85 and -70 meV for Ar on noble metals. Note, however, that Cheng *et al.*⁴⁵ adopted an effective-medium theory that is not able to discriminate between different adsorption sites; moreover, a simple Lennard-Jones potential is expected to always predict the hollow site as the preferred one for Ar on noble metals, in contrast to both the experimental evidence and the present results.

As expected, we find that for adsorption on both Cu(111) and Pb(111), the binding energy increases by going from Ne to Xe, in line with the increasing polarizability of this atom sequence. In particular, for several close-packed transition-metal surfaces the binding energy of Xe is found⁹ to be about two to three times larger than that of Kr and Ar, respectively, a behavior that is well reproduced by our DFT/vdW-WF method [the factors are 1.5 and 3 for adsorption on Cu(111) and 1.6 and 2.5 for adsorption on Pb(111)]. This general behavior is also in line with the results of Zhang *et al.*¹⁶

Our energetic results are not far from the best estimate reported by Vidali *et al.*² for Xe on Cu(111), i.e., a binding energy of -183 ± 10 meV at a distance of 3.60 ± 0.08 Å (these values represent averages over different theoretical/experimental estimates). In their tables Vidali *et al.*² also report for Ar on Cu(111) a binding energy of -85 meV at a distance of 3.53 Å and for Kr on Cu(111) a binding energy of -119 meV, in fair agreement with our results. Lazic *et al.*¹¹ studied the adsorption of Xe on Cu(111) by a DFT approach where vdW corrections were included using the method of Andersson *et al.*,²⁶ using the PW91 and PBE functionals as reference DFT functionals (see the last column in Tables I and IV). As can be seen, our results are much closer to the experimental estimate than those of Lazic *et al.*,¹¹ which tend to overestimate the binding energy and underestimate the equilibrium distance. The Xe-adsorbed Cu(111) surface has been also recently investigated by Sun and Yamauchi¹³ using DFT with semiempirical vdW corrections. They found reasonable equilibrium distances; however, the computed binding energy was greatly overestimated (it was even larger than that obtained by the LDA) and the favored adsorption site was incorrectly predicted to be the hollow site, probably due to the use of semiempirical pair potentials that favor close-packed structures and high-coordinated sites (see the discussion above).

From Tables I, III, and IV, one can also see that the binding energies are reasonably reproduced by the LDA scheme for RGs on Cu(111), a behavior common to several physisorption systems. However, as already outlined above, this agreement should be considered accidental: The well-known LDA overbinding, due to the overestimation of the long-range part of the exchange contribution, somehow mimics the missing vdW interactions; the equilibrium distances predicted by the LDA are clearly underestimated since the LDA cannot reproduce the R^{-6} behavior in the interaction potential. For RGs on Pb(111), the LDA binding energies are instead underestimated as a

consequence (as discussed above) of the larger equilibrium distances than for RGs on Cu(111).

As already found elsewhere,^{8,9} for all the used schemes, the binding energies correlate with the RG metal distance: In fact, for a given RG, the configurations having the strongest binding are characterized by the shortest RG-substrate distance. Moreover, all the methods predict that Ar and Xe adatoms get closer to the Cu(111) surface when adsorbed on the top site, as found in several previous studies.^{8,9,12} Remarkably, this behavior cannot be reproduced^{6,9} using a hard-sphere model, indicating that there is a significant interaction between the Ar and Xe atoms and the Cu(111) surface so that a simple stacking (hard-sphere) model of weakly or noninteracting spheres is not valid (for comparison, in Tables IV and V we also list the sums of the RG atoms and metal atom vdW literature radii). Instead, for adsorption on Pb(111), the adatoms in the hollow site are closer to the surface than in the top one, in line with the usual behavior. These results can be easily elucidated by analyzing the parameters of the adopted fitting function (see above) $A e^{-Bz} - C_3/(z - z_0)^3$: We find that, as a general rule, at the equilibrium distance, the repulsive potential term is weaker on the favored adsorption site [for instance, the top site for Xe on Cu(111) and the hollow one for Xe on Pb(111)], in agreement with the results of Da Silva *et al.*⁸

From our fitted binding-energy curves it is possible in principle to get estimates of the long-range C_3 coefficients. However, a quantitative characterization of the long-range asymptotic part of the interaction (where the binding energy is quite small) is not easy and represents a notoriously difficult problem.¹ In fact, one typically finds a significant discrepancy between C_3 values obtained when the fitting parameters are set to reproduce the interaction near the minimum and those computed considering the asymptotic region only. For instance, considering Ar on Cu(111) (in the top adsorption site), from the fitting of the whole binding-energy curve we estimate $C_3 = 3942$ meV Å³, while, if the fit is restricted to the points corresponding to the largest Ar-surface distances, $C_3 = 2692$ meV Å³, in better agreement with (but still overestimated with respect to) the reference value² $C_3 = 1621$ meV Å³. In most of the first-principles studies (including ours) on adsorption processes, where the substrate is modeled by a slab made of a few atomic layers, the focus is mainly on the equilibrium properties, corresponding to a region not far from the minimum of the binding-energy curve. The asymptotic behavior is instead typically studied by adopting empirical interaction potentials or simplified jellium models for the surfaces (see, for instance, Ref. 46). Preliminary test calculations to get better estimates for the C_3 coefficients are reported in Ref. 47.

Ferralis *et al.*¹⁵ studied the structural and thermal properties of Xe on the Pb(111) surface by LEED. They observed the formation of a Xe monolayer with an incommensurate hexagonal structure with a lattice parameter similar to that found in bulk Xe (4.33 Å); this structure is aligned with the substrate lattice but has a larger unit cell, similarly to the case of Xe on Ag(111), which is also an aligned incommensurate monolayer. They also found that the heat of adsorption for the first Xe layer is -191 ± 10 meV with an overlayer-substrate spacing of 3.95 ± 0.10 Å. Looking at Table III we found that our computed E_a (-205.5 meV for the hollow adsorption site)

TABLE V. Equilibrium RG adatom-surface distance (in angstroms) on the Pb(111) surface computed using the standard DFT PW91 calculation and including the vdW corrections using our DFT/vdW-WF method compared to the LDA result, the vdW-DF method by Dion *et al.* (Ref. 41) compared to the LDA result, and available theoretical and available theoretical and experimental (in parentheses) reference data; the sum s of the vdW radii of the RG atom and the Pb atom is also reported.

System	PW91	DFT/vdW-WF	LDA	vdW-DF	Reference data	s
Ne-Pb(111) hollow	3.80	3.41	3.10	3.70	3.5 ^a	3.56
Ne-Pb(111) top	4.00	3.68	3.40	3.90	3.8 ^a	3.56
Ne-Pb(111) bridge	3.80	3.36	3.27	3.50		3.56
Ar-Pb(111) hollow	4.40	3.68	3.40	4.00		3.90
Ar-Pb(111) top	4.40	4.04	3.60	4.22		3.90
Ar-Pb(111) bridge	4.50	3.77	3.43	4.10		3.90
Kr-Pb(111) hollow	4.40	3.69	3.40	4.14	3.8 ^a	4.04
Kr-Pb(111) top	4.40	3.98	3.70	4.24	3.9 ^a	4.04
Kr-Pb(111) bridge	4.30	3.79	3.51	4.13		4.04
Xe-Pb(111) hollow	4.30	3.93	3.50	4.30	(3.95 ^b)	4.18
Xe-Pb(111) top	4.50	4.02	3.70	4.30		4.18
Xe-Pb(111) bridge	4.70	3.93	3.55	4.31		4.18

^aReference 16.

^bReference 15.

is close to the experimental value and in better agreement than with the other methods, although our model structure is not exactly the same observed experimentally. Moreover, also the Xe-Pb(111) distance (3.93 Å) is in excellent agreement (see Table V) with that estimated by Ferralis *et al.*,¹⁵ which gives further support to the reliability of our DFT/vdW-WF method. As expected, it has been found¹⁵ that a hard-sphere model is unable to give a good description of adsorption of Xe on Pb(111). For Xe-Pb(111) the heat of adsorption is lower than for Xe on any surface measured so far,¹⁵ with the possible exception of Al(110) and for alkali metals; a low heat of adsorption is not particularly surprising since the Pb atoms are much larger than most other metals (the vdW radius of Pb is 2.02 Å, compared to 1.72 Å for Ag, 1.72 Å for Pt, 1.63 Å for Pd, and 1.40 Å for Cu), implying that the repulsive Xe-Pb interaction prevents the Xe from approaching the deeper part of the attractive holding potential. It must be noted that Ferralis *et al.*¹⁵ were unable to determine the preferred adsorption site, the lack of satellite intensities in the LEED patterns indicating that the overlayer is quite uniform and the corrugation is small.

An important quantity that often provides revealing details of the bonding mechanism in adsorption processes is represented by the electron-density difference $\Delta n(\mathbf{r}) = n_{\text{RG}/s}(\mathbf{r}) - n_s(\mathbf{r}) - n_{\text{RG}}(\mathbf{r})$, obtained from the electron density (at the equilibrium geometry) of the RG on the substrate, of the clean substrate and the isolated RG monolayer, respectively. Our approach in this respect is not fully self-consistent because we use the electron density obtained at a pure PW91 level, that is, without vdW corrections; however, the effects due to the lack of self-consistency are expected to be negligible because the rather weak and diffuse vdW interactions should not substantially change the electronic charge distribution.⁴⁸ Plots of $\Delta n(\mathbf{r})$ for Xe on Cu(111) and Xe on Pb(111), in both the hollow and top sites (see Figs. 3 and 4), show that, in agreement with what was found previously⁹ for RGs on Pd(111), the electron-density redistribution is stronger on the Cu atoms for the Xe on the top site than for the hollow site; both sites exhibit a significant depletion of electron

density centered about the Xe atom together with a slight density accumulation close to the center of the Xe atom, this effect being attributed⁹ to orthogonalization of Xe states to the states of the substrate atoms. Moreover, for Xe in the on-top site, there is a significant electron-density accumulation between the Xe atom and the topmost surface layer. Note that, there is a clear tendency of Xe to induce a much larger charge delocalization on the Cu(111) surface than on Pb(111), in line with the delocalization mechanism invoked^{6,18} to explain the preference for the top adsorption site on Cu(111). Note that, Chen *et al.*,¹⁴ who studied Xe on Cu(111) using the vdW-DF approach in the more recent variant,⁴⁹ suggest that a key role in the determination of the preferred adsorption site is played by the interaction between the p electrons of the RG atoms and the d electrons of the transition metal surface; in particular, hollow sites are preferred for Pb(111) because the Pb d orbitals are completely filled.

Since polarization effects are assumed to play a key role in determining the favored adsorption sites,^{9,12} we have also computed the change of the work function ΔW of the Cu(111) and Pb(111) substrate upon adsorption of RG atoms. The work functions have been calculated as the difference between the average electrostatic Coulomb potential at the midpoint of the vacuum region of the slab and the Fermi energy:⁵⁰ For the clean Cu(111) and Pb(111) surfaces we estimate a work function of 4.85 and 3.86 eV, respectively, in excellent agreement with the reference values, which are in the range from 4.90 to 5.01 eV for Cu(111) (Ref. 51) and 3.83 eV for Pb(111).⁵² The change of the work function ΔW can be related to the dipole moment induced in the substrate by the presence of the RG adatom $\Delta\mu$ using the Helmholtz equation⁵³

$$\Delta\mu = \frac{1}{12\pi} \frac{A_{(1\times 1)}}{\Theta} \Delta W, \quad (6)$$

where $A_{(1\times 1)}$ is the area of the (1×1) surface unit cell (in Å²) and Θ is the RG coverage; if ΔW is given in eV, then $\Delta\mu$ is in debyes. In our case $\Theta = 1/3$, so that $\Delta\mu = \sqrt{3}a_0^2/16\pi \Delta W$, where a_0 is the Cu or Pb lattice constant. Our computed

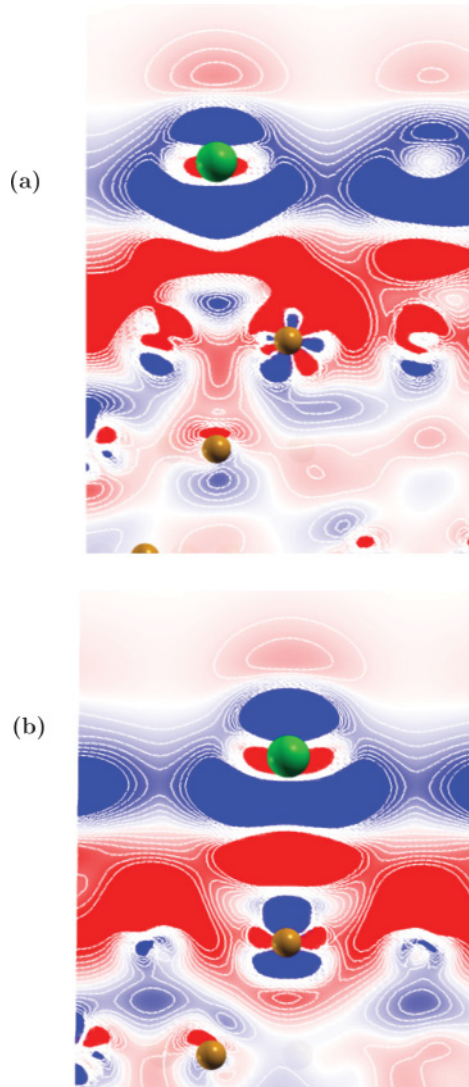


FIG. 3. (Color online) Electron-density difference of Xe on Cu(111) in the (a) hollow and (b) top sites shown in a plane perpendicular to the surface, within the range of $\pm 1 \times 10^{-4} e/\text{bohr}^3$. Light gray (red) and dark gray (blue) represent electron accumulation and depletion, respectively. The green and orange spheres indicate the Xe and Cu atoms, respectively.

ΔW and $\Delta\mu$ values are listed in Table VI. In agreement with previous *ab initio* calculations,^{8,9} we find that the RG adsorption induces a decrease in the work function, thus indicating that the RG atoms behave as adsorbates with an effective positive charge; note that this is consistent with the depletion of the electron density about the Xe atom discussed above, which corresponds to an induced surface dipole moment that points out of the surface. For Xe on Cu(111) our estimated ΔW and $\Delta\mu$ values (see Table VI) agree well with the experimental estimates⁵⁴ of -0.60 eV and -0.24 D, respectively. As can be seen in Table VI, the absolute value of $\Delta\mu$ increases from Ne to Xe, because the corresponding electronic polarizabilities increase, and is larger for the optimal adsorption site, for instance, the top site for Xe on Cu(111) and the hollow site for Xe on Pb(111). Moreover, it is considerably larger on Cu(111) than on Pb(111), in line with

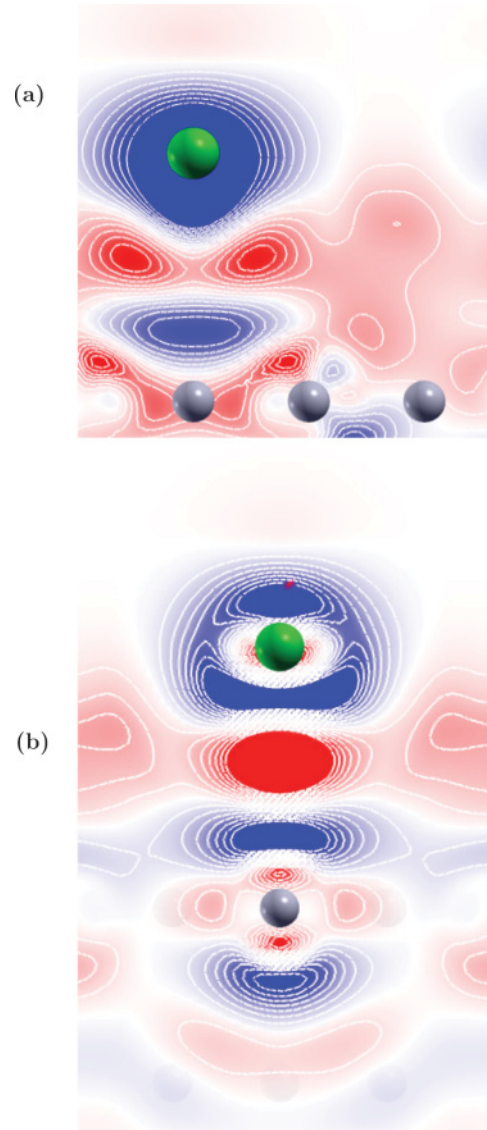


FIG. 4. (Color online) Electron-density difference of Xe on Pb(111) in the (a) hollow and (b) top sites shown in a plane perpendicular to the surface, within the range of $\pm 1 \times 10^{-4} e/\text{bohr}^3$. Light gray (red) and dark gray (blue) represent electron accumulation and depletion, respectively. The green and gray spheres indicate the Xe and Pb atoms, respectively.

TABLE VI. Work-function change (in eV) and induced dipole moment (in parentheses) (in debyes) for RGs adatoms on the Cu(111) and Pb(111) surfaces at equilibrium geometries.

System	Hollow	Top
Ne-Cu(111)	-0.04 (-0.02)	-0.03 (-0.01)
Ar-Cu(111)	-0.28 (-0.13)	-0.37 (-0.17)
Kr-Cu(111)	-0.54 (-0.24)	-0.37 (-0.17)
Xe-Cu(111)	-0.53 (-0.24)	-0.57 (-0.26)
Ne-Pb(111)	-0.03 (-0.03)	-0.03 (-0.03)
Ar-Pb(111)	-0.10 (-0.08)	-0.03 (-0.03)
Kr-Pb(111)	-0.11 (-0.09)	-0.05 (-0.04)
Xe-Pb(111)	-0.13 (-0.11)	-0.04 (-0.03)

the energy analysis reported above, which indicated a stronger interaction of RGs with the Cu(111) surface than with Pb(111).

Zhang *et al.*¹⁶ explain the much larger mobility of Ne overlayers on Pb(111), as observed in friction experiments, than of Kr overlayers on the basis of the different activation energies that characterize the lateral motion of Ne and Kr atoms on the Pb(111) surface. The activation energies for a monolayer can be directly calculated from the difference in the binding energy of the adatom between the favored (hollow) site and the transition state, which is expected to correspond to the bridge site.¹⁶ Considering the differences between the binding energy of the hollow and bridge configurations for Ne and Kr on Pb(111), we qualitatively confirm the trend observed by Zhang *et al.*,¹⁶ since our estimated activation energies (1.3 meV for Ne and 6.0 meV for Kr) are of the same order of magnitude as those reported in Ref. 16 (0.7 meV for Ne and 2.5 meV for Kr). However, such small energy values are comparable to (or even smaller than) the expected accuracy of the computed binding energies, thus making quantitative estimates of the hopping probabilities¹⁶ (which depend exponentially on the aforementioned activation energies) rather questionable.

IV. CONCLUSION

In summary, by analyzing the results of our study of the adsorption of RG atoms on the Cu(111) and Pb(111) surfaces, one can conclude that the inclusion of the vdW corrections by the DFT/vdW-WF method systematically improves upon the estimates for the binding energies as obtained by a standard

GGA approach. In particular, using a pure PW91 functional, the binding is underestimated in all cases, while equilibrium distances are overestimated. For all the system considered the vdW correction term represents the dominant part of the binding energy, although, particularly for RG adsorption on Pb(111), the pure PW91 approach gives a substantial contribution. However, vdW interactions appear not to play a critical role in the adsorption site preference [the same result has been obtained by Zhang *et al.*¹⁶ studying the interaction of Ne and Kr on Pb(111)]: Xe on Cu(111) clearly prefers the top site, while for Ne, Ar, and Kr on Cu(111) the differences in binding energies relative to different adsorption sites are so small that is not easy to attribute a definitive preference; instead, the hollow configuration tends to be preferred for adsorption of all the considered RGs on Pb(111), in agreement with previous calculations and experimental observations.^{15,16} Moreover, the Pb(111) substrate is subject, upon rare-gas adsorption, to a significantly smaller change in the work function and to a correspondingly smaller (in absolute value) induced dipole moment than Cu(111). Given these relevant peculiarities of the Pb(111) surface, where the hollow site is undoubtedly favored for adsorption of RG atoms, this surface would represent an ideal substrate to study, both theoretically and experimentally, high-coordination adsorption sites.

ACKNOWLEDGMENTS

We thank very much F. Costanzo, G. Mistura, and F. Toigo for useful discussions.

*Present address: Center for Chemistry, Institute of Chemistry, Technology and Metallurgy, University of Belgrade, Njegoševa 12, 11001, Belgrade, Serbia and Scuola Normale Superiore, piazza dei Cavalieri 7, I-56126 Pisa, Italy.

¹L. W. Bruch, M. W. Cole, and E. Zaremba, *Physical Adsorption: Forces and Phenomena* (Clarendon, Oxford, 1997).

²G. Vidali, G. Ihm, H. Y. Kim, and M. W. Cole, *Surf. Sci. Rep.* **12**, 133 (1991).

³J. M. Gottlieb, *Phys. Rev. B* **42**, 5377 (1990).

⁴Th. Seyller, M. Caragiu, R. D. Diehl, P. Kaukasoina, and M. Lindroos, *Chem. Phys. Lett.* **291**, 567 (1998); M. Caragiu, Th. Seyller, and R. D. Diehl, *Phys. Rev. B* **66**, 195411 (2002).

⁵B. Narloch and D. Menzel, *Chem. Phys. Lett.* **290**, 163 (1997).

⁶R. D. Diehl, Th. Seyller, M. Caragiu, G. S. Leatherman, N. Ferralis, K. Pussi, P. Kaukasoina, and M. Lindroos, *J. Phys.: Condens. Matter* **16**, S2839 (2004).

⁷J. L. F. Da Silva, C. Stampfl, and M. Scheffler, *Phys. Rev. Lett.* **90**, 066104 (2003).

⁸J. L. F. Da Silva, C. Stampfl, and M. Scheffler, *Phys. Rev. B* **72**, 075424 (2005).

⁹J. L. F. Da Silva and C. Stampfl, *Phys. Rev. B* **77**, 045401 (2008).

¹⁰A. E. Betancourt and D. M. Bird, *J. Phys.: Condens. Matter* **12**, 7077 (2000).

¹¹P. Lazić, Z. Crljen, R. Brako, and B. Gumhalter, *Phys. Rev. B* **72**, 245407 (2005).

¹²M. C. Righi and M. Ferrario, *J. Phys.: Condens. Matter* **19**, 305008 (2007).

¹³X. Sun and Y. Yamauchi, *J. Appl. Phys.* **110**, 103701 (2011).

¹⁴D.-L. Chen, W. A. Al-Saidi, and J. K. Johnson, *Phys. Rev. B* **84**, 241405(R) (2011).

¹⁵N. Ferralis, H. I. Li, K. J. Hanna, J. Stevens, H. Shin, F. M. Pan, and R. D. Diehl, *J. Phys.: Condens. Matter* **19**, 056011 (2007).

¹⁶Y. N. Zhang, F. Hanke, V. Bortolani, M. Persson, and R. Q. Wu, *Phys. Rev. Lett.* **106**, 236103 (2011).

¹⁷L. Bruschi, M. Pierno, G. Fois, F. Ancilotto, G. Mistura, C. Boragno, F. Buatier de Mongeot, and U. Valbusa, *Phys. Rev. B* **81**, 115419 (2010).

¹⁸P. S. Bagus, V. Staemmler, and C. Wöll, *Phys. Rev. Lett.* **89**, 096104 (2002).

¹⁹See, for instance, W. Kohn, Y. Meir, and D. E. Makarov, *Phys. Rev. Lett.* **80**, 4153 (1998).

²⁰R. Eisenhitz and F. London, *Z. Phys.* **60**, 491 (1930).

²¹K. E. Riley, M. Pitonák, P. Jurecka, and P. Hobza, *Chem. Rev.* **110**, 5023 (2010).

²²A. Tkatchenko, L. Romaner, O. T. Hofmann, E. Zojer, C. Ambrosch-Draxl, and M. Scheffler, *MRS Bull.* **35**, 435 (2010).

²³P. L. Silvestrelli, *Phys. Rev. Lett.* **100**, 053002 (2008).

²⁴P. L. Silvestrelli, K. Benyahia, S. Grubisić, F. Ancilotto, and F. Toigo, *J. Chem. Phys.* **130**, 074702 (2009).

²⁵P. L. Silvestrelli, *J. Phys. Chem. A* **113**, 5224 (2009).

²⁶Y. Andersson, D. C. Langreth, and B. I. Lundqvist, *Phys. Rev. Lett.* **76**, 102 (1996).

²⁷N. Marzari and D. Vanderbilt, *Phys. Rev. B* **56**, 12847 (1997).

²⁸P. L. Silvestrelli, *Chem. Phys. Lett.* **475**, 285 (2009).

- ²⁹P. L. Silvestrelli, F. Toigo, and F. Ancilotto, *J. Phys. Chem. C* **113**, 17124 (2009).
- ³⁰A. Ambrosetti and P. L. Silvestrelli, *J. Phys. Chem. C* **115**, 3695 (2011).
- ³¹S. Baroni *et al.* [www.quantum-espresso.org].
- ³²WANT code by A. Ferretti *et al.* [www.wannier-transport.org].
- ³³E. Abad, Y. J. Dappe, J. I. Martinez, F. Flores, and J. Ortega, *J. Chem. Phys.* **134**, 044701 (2011).
- ³⁴J. P. Perdew and Y. Wang, *Phys. Rev. B* **45**, 13244 (1992).
- ³⁵J. P. Perdew, K. Burke, and M. Ernzerhof, *Phys. Rev. Lett.* **77**, 3865 (1996).
- ³⁶Y. Zhang and W. Yang, *Phys. Rev. Lett.* **80**, 890 (1998).
- ³⁷R. R. Rehr, E. Zaremba, and W. Kohn, *Phys. Rev. B* **12**, 2062 (1975); J. Tao, J. P. Perdew, and A. Ruzsinszky, *ibid.* **81**, 233102 (2010).
- ³⁸E. M. Lifshitz, *Sov. Phys. JETP* **2**, 73 (1956); E. Zaremba and W. Kohn, *Phys. Rev. B* **13**, 2270 (1976).
- ³⁹V. G. Ruiz, W. Liu, E. Zojer, M. Scheffler, and A. Tkatchenko, *Phys. Rev. Lett.* (to be published).
- ⁴⁰K. Lee, Y. Morikawa, and D. C. Langreth, *Phys. Rev. B* **82**, 155461 (2010).
- ⁴¹M. Dion, H. Rydberg, E. Schröder, D. C. Langreth, and B. I. Lundqvist, *Phys. Rev. Lett.* **92**, 246401 (2004); G. Roman-Perez and J. M. Soler, *ibid.* **103**, 096102 (2009).
- ⁴²A. Tkatchenko and O. A. von Lilienfeld, *Phys. Rev. B* **73**, 153406 (2006).
- ⁴³L. Sheng, Y. Ono, and T. Taketsugu, *J. Phys. Chem. C* **114**, 3544 (2010).
- ⁴⁴M. Vanin, J. J. Mortensen, A. K. Kelkkanen, J. M. Garcia-Lastra, K. S. Thygesen, and K. W. Jacobsen, *Phys. Rev. B* **81**, 081408 (2010).
- ⁴⁵E. Cheng, M. W. Cole, W. F. Saam, and J. Treiner, *Phys. Rev. B* **48**, 18214 (1993).
- ⁴⁶E. Hult, H. Rydberg, B. I. Lundqvist, and D. C. Langreth, *Phys. Rev. B* **59**, 4708 (1999).
- ⁴⁷A. Ambrosetti and P. L. Silvestrelli, *Phys. Rev. B* **85**, 073101 (2012).
- ⁴⁸T. Thonhauser, V. R. Cooper, S. Li, A. Puzder, P. Hyldgaard, and D. C. Langreth, *Phys. Rev. B* **76**, 125112 (2007).
- ⁴⁹K. Lee, É. D. Murray, L. Kong, B. I. Lundqvist, and D. C. Langreth, *Phys. Rev. B* **82**, 081101(R) (2010).
- ⁵⁰C. J. Fall, N. Binggeli, and A. Baldereschi, *J. Phys.: Condens. Matter* **11**, 2689 (1999).
- ⁵¹C. J. Fall, N. Binggeli, and A. Baldereschi, *Phys. Rev. B* **61**, 8489 (2000).
- ⁵²B. Sun, P. Zhang, Z. Wang, S. Duan, X.-G. Zhao, X. Ma, and Q.-K. Xue, *Phys. Rev. B* **78**, 035421 (2008).
- ⁵³L. D. Schmidt and R. Gomer, *J. Chem. Phys.* **45**, 1605 (1966).
- ⁵⁴P. Zeppenfeld, in *Physics of Covered Solid Surfaces*, edited by H. P. Bonzel, Landolt-Börnstein, New Series, Group III, Vol. 42, Pt. A (Springer-Verlag, Berlin, 2001), p. 67.